Organic LETTERS

Letter

pubs.acs.org/OrgLett

Hyalachelins A–C, Unusual Siderophores Isolated from the Terrestrial Myxobacterium *Hyalangium minutum*

Suvd Nadmid,[†,‡] Alberto Plaza,[†,‡] Gianluigi Lauro,[§] Ronald Garcia,[†,‡] Giuseppe Bifulco,*[,§] and Rolf Müller*[,†,‡]

[†]Department of Microbial Natural Products, Helmholtz-Institute for Pharmaceutical Research Saarland (HIPS), Helmholtz Centre for Infection Research (HZI) and Pharmaceutical Biotechnology, Saarland University, Campus C2 3, 66123 Saarbrücken, Germany

[‡]German Center for Infection Research (DZIF), Partner site Hannover-Braunschweig, 38124 Braunschweig, Germany

[§]Dipartimento di Farmacia, Università degli Studi di Salerno, via Giovanni Paolo II 132, 84084, Fisciano (SA), Italy

Supporting Information

ABSTRACT: Three new siderophores, termed hyalachelins A–C (**1**–**3**), were isolated from the terrestrial myxobacterium *Hyalangium minutum*. Their structures were determined by 2D NMR and HR-MS/MS experiments, and their stereochemical configuration was established by a combination of NMR data, quantum mechanical calculations, and circular dichroism experiments. Hyalachelins are unusual catecholate-type siderophores that bear a 3,7,8-trihydroxy-1-oxo-1,2,3,4-tetrahydroisoquinoline-3-carboxylic acid. Their iron chelating activities were evaluated in a CAS assay showing EC_{50} values of ~30 μM.

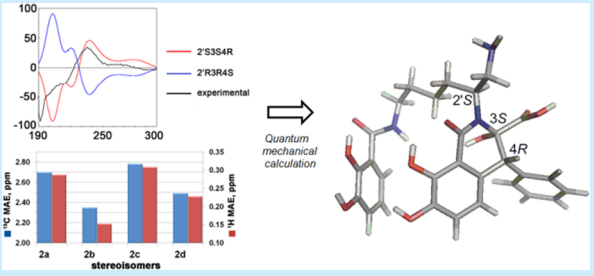

Most bacteria require iron for growth. In response to iron limitation which is caused by low solubility of Fe^{3+} at physiological pH, bacteria produce and secrete iron chelating small molecules, termed siderophores. The siderophore–iron complex exhibits improved solubility and enables the transport of ferric iron into the cell through outer-membrane receptor proteins.[1,2] To date only two different structural classes of siderophores, the catecholates myxochelin A and B,[3,4] and the citrate-hydroxamates nannochelins,[5] have been reported from myxobacteria.

Over the course of our research aimed at the discovery of new bioactive natural products from myxobacteria by using NMR and MS profiling,[6] our attention was drawn to screen novel and unexplored strains, which led to the isolation of new structural varieties.[7,8] Strain MCy9135 was isolated from a soil sample collected in Xiamen, China, and it is phenotypically and phylogenetically related to the unexplored species *Hyalangium minutum* by 16S rDNA analysis. An ethyl acetate extract of the strain MCy9135 was analyzed by LC-MS and LC-NMR and revealed the presence of four different classes of natural products, including three new catecholate siderophores, termed hyalachelins A–C (**1**–**3**, Figure 1), together with the known tartrolon D,[9] myxochelin B,[4] and hyafurones.[10]

Hyalachelin A (**1**) was isolated as a colorless amorphous solid. Its molecular formula was determined to be $C_{29}H_{32}N_3O_{10}$, based on a molecular ion at m/z 582.2074 $[M + H]^+$observed in HR-ESI-MS (calculated 582.2088, Δppm 2.4), requiring 16 degrees of unsaturation. The ^{1}H NMR spectrum of **1** in CD_3OD (Table 1) exhibited aromatic proton signals including two doublets at δ 7.17 (2H, d, J = 8.5 Hz) and 6.72 (2H, d, J = 8.5 Hz) corresponding to a *para*-substituted aromatic ring and a pair of

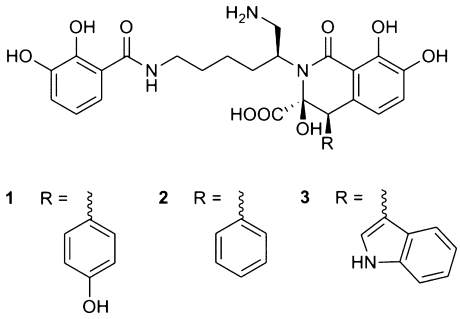

Figure 1. Hyalachelins A–C (**1**–**3**).

doublets at δ 6.80 (1H, d, J = 8.2 Hz) and 6.12 (1H, d, J = 8.2 Hz), characteristic of a tetrasubstituted benzene ring. Moreover, a set of signals comprising two doublets at δ 7.17 (1H, d, J = 8.0 Hz), 6.90 (1H, dd, J = 8.0, 1.0 Hz) and a triplet at δ 6.68 (1H, t, J = 8.0 Hz) were observed and suggested the presence of a 1,2,3-trisubstituted benzene ring. Examination of the HSQC spectrum revealed the presence of two methines ($\delta_{C\text{-}4}$ 52.2, $\delta_{H\text{-}4}$ 4.70; $\delta_{C\text{-}2'}$ 59.6, $\delta_{H\text{-}2'}$ 3.51) and two aminomethylenes ($\delta_{C\text{-}1'}$ 41.3, $\delta_{H\text{-}1'}$ 3.87, 3.13; $\delta_{C\text{-}6'}$ 40.1, $\delta_{H\text{-}6'}$ 3.36, 3.31).

Analysis of TOCSY and COSY cross peaks yielded four spin systems, three of which comprise aromatic protons. HMBC and HSQC correlations together with splitting patterns of the aromatic protons at δ 6.12–7.17 were indicative of two 2,3-dihydroxybenzoyl moieties (DHB-1 and DHB-2, respectively)

Received: June 24, 2014
Published: July 24, 2014

   dx.doi.org/10.1021/ol501826a | *Org. Lett.* 2014, 16, 4130–4133

Table 1. NMR Spectroscopic Data for Hyalachelin A (1) in CD_3OD

pos	δ_H,[a] mult (J in Hz)	δ_C[b]	HMBC[c]
1		172.3	
2			
3		94.3	
4	4.70, s	52.2	3, 5, 6, 10, 11, 1‴, 2‴
5		132.1	
6		113.0	
7		150.6	
8		145.3	
9	6.80, d (8.2)	120.1	5, 7, 8
10	6.12, d (8.2)	118.4	1, 4, 6, 7, 8
11		175.2	
1′a	3.87, t (11.7)	41.3	2′
1′b	3.13, dd (12.5, 3.3)		
2′	3.51, m	59.6	1, 3, 1′, 3′, 4′
3′a	2.16, m	31.5	1′, 2′, 4′, 5′
3′b	2.03, m		2′, 4′
4′a	1.41, m	25.1	2′, 3′, 6′
4′b	1.36, m		
5′	1.60, m	30.0	3′, 4′, 6′
6′a	3.36, m	40.1	4′, 5′, 7″
6′b	3.31, m		
1″		116.5	
2″		150.1	
3″		147.0	
4″	6.90, dd (8.0, 1.0)	119.3	2″, 3″, 6″
5″	6.68, t (8.0)	119.3	1″, 3″, 6″
6″	7.17, d (8.0)	118.4	1″, 2″, 4″, 5″, 7″
7″		171.2	
1‴		128.4	
2‴, 6‴	7.17, d (8.5)	133.4	4, 1‴, 4″
3‴, 5‴	6.72, d (8.5)	115.6	1‴, 4‴
4‴		157.8	

[a]Recorded at 700 MHz, referenced to residual CD_3OD at δ 3.31 ppm. [b]Recorded at 175 MHz, referenced to residual CD_3OD at δ 49.15 ppm. [c]Proton showing HMBC correlation to indicated carbon.

and a phenol moiety. Finally, the last spin system comprising protons H-1′ to H-6′ was deduced as a hexane-1,2,6-triamine moiety. A long-range correlation from the proton at δ 3.36 (H-6′a) to the carbonyl resonance at δ 171.2 linked the triamine moiety to DHB-1 forming the partial structure A (Figure 2). Partial structure B was assembled on the basis of HMBC correlations. In particular, key correlations from the methine proton H-4 to the aromatic carbons at δ 132.1 (C-5), 113.0 (C-6), 118.4 (C-10), and 133.4 (C-2‴) connected DHB-2 to the

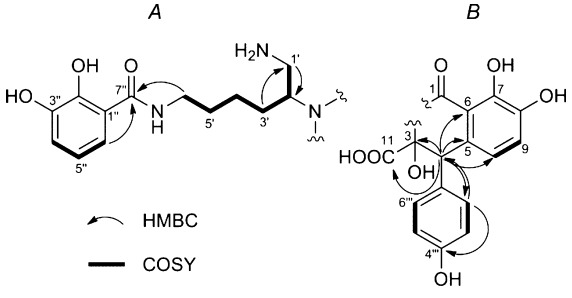

Figure 2. Selected key HMBC and COSY correlations for fragment A and B of hyalachelin A (**1**).

phenol residue via the methine at C-4. ROESY correlations from H-10 to H-4 and H-2‴ supported this connectivity (Figure 3).

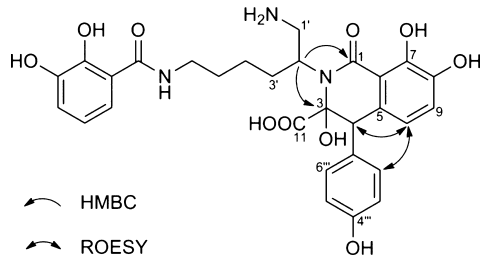

Figure 3. Key HMBC correlations used to link two fragments and ROESY correlations.

Further HMBC correlations from H-4 to the carbon resonances at δ 94.3 (C-3) and 175.2 (C-11) attached C-4 to the α-hydroxy acid at C-3, completing the partial fragment B as depicted in Figure 2.

Inspection of the partial fragments A and B revealed that together they contained 15 of the required 16 degrees of unsaturation indicating that linkage between fragments A and B involved formation of a ring to satisfy the unsaturation index and the molecular formula. HMBC correlations from H-2′ to the carbon resonances at δ 172.3 (C-1) and 94.3 (C-3) linked fragments A and B, which form a six-membered ring containing both an amide and a hemiaminal functional group. Therefore, the structure of **1** was established as a linear catecholate siderophore that contains a hexasubstituted tetrahydroisoquinoline ring linked to a phenol moiety at position 4.

Tandem mass spectrometry provided further evidence to support the structure of **1**. The MS^2 fragmentation of the major ion peak at m/z 582 $[M + H]^+$ displayed an intense ion at m/z 564 $[M + H - H_2O]^+$. MS of the daughter ion peak displayed a predominant fragment at m/z 503 $[M + H - H_2O - 44 - 17]^+$ corresponding to the loss of CO_2 and NH_2. Finally, MS^4 fragmentation of this ion peak produced a fragment ion at m/z 367 $[M + H - H_2O - 44 - 17 - 136]^+$ corresponding to the loss of a DHB residue along with an ion peak at m/z 270 $[M + H - H_2O - 44 - 17 - 233]^+$ corresponding to the loss of fragment A (Figure S1). Thus, the MS^n fragmentation patterns were in complete agreement with the structure of **1** as determined by NMR.

HR-ESI-MS analysis of hyalachelin B (**2**) showed a molecular ion peak at m/z 566.2127 $[M + H]^+$ appropriate for a molecular formula of $C_{29}H_{32}N_3O_9$ (calculated 566.2139, Δppm 2.12), which is 16 mass units lower than that of **1**. The 2D NMR data for **2** closely resembled those of **1** with the exception that resonances belonging to the phenol of **1** were replaced by resonances belonging to a phenyl group in **2**.

Hyalachelin C (**3**) showed a molecular ion peak at 605.2235 $[M + H]^+$ observed in HR-ESI-MS (calculated 605.2248, Δppm 2.15), which corresponded to a molecular formula of $C_{31}H_{33}N_4O_9$. The ^1H NMR spectrum exhibited significant differences in the downfield region in comparison to that of **1**, displaying proton signals consistent with the presence of an indole ring. On the basis of the 2D NMR data **3** was identified as the indole-derivative of **1**.

Due to the lack of possible diagnostic ROE effects in the cyclic and flexible portions of the molecule, the relative configuration of representative hyalachelin B (**2**) was assigned by quantum mechanical calculations of ^{13}C and ^1H NMR chemical shifts.[11,12] By using Monte Carlo Molecular Mechanics (MCMM) and

dx.doi.org/10.1021/ol501826a | Org. Lett. 2014, 16, 4130−4133

Molecular Dynamics (MD) simulations, an extensive conformational search at the empirical level was performed for each of the four possible relative stereoisomers (Figure S3), termed **2a** (2′*S**,3*R**,4*R**), **2b** (2′*S**,3*S**,4*R**), **2c** (2′*S**,3*R**,4*S**), and **2d** (2′*S**,3*S**,4*S**). All the nonredundant conformers were subsequently geometry and energy optimized at the density functional level (DFT) using the MPW1PW91 functional and 6-31G(d) basis set and using IEFPCM for simulating the DMSO solvent (Gaussian 09 software package).[13] On the previously optimized geometries of all four possible relative stereoisomers (**2a**−**d**), we performed quantum mechanical calculations of ^{1}H and ^{13}C NMR chemical shifts (Tables S5 and S6) and compared them to the experimental data in order to have indications on the relative configuration of **2**. The mean absolute error (MAE) value was used to impartially compare calculated and experimental ^{1}H and ^{13}C NMR chemical shifts (Figure 4). Indeed, isomer **2b**

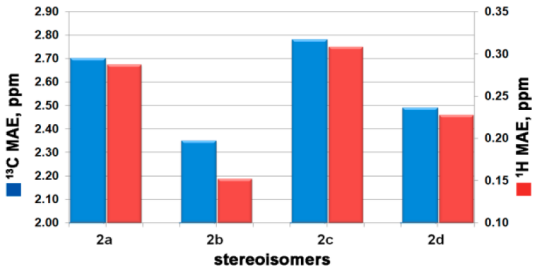

Figure 4. Mean absolute error (MAE) histograms obtained by comparison of the ^{13}C (blue bars) and ^{1}H (red bars) chemical shifts for stereoisomers **2a**, **2b**, **2c**, and **2d** with the experimental data. MAE = $\Sigma[|(\delta_{exp} - \delta_{calcd})|]/n$, summation through n of the absolute error values (difference of the absolute values between corresponding experimental and calculated ^{13}C, ^{1}H chemical shifts), normalized to the number of the chemical shifts considered. The lowest MAE is reflected by the **2b** relative stereoisomer.

displayed the lowest MAE values (^{13}C MAE = 2.35 ppm, ^{1}H MAE = 0.15 ppm) suggesting that the relative configuration of **2** is 2′*S**,3*S**,4*R**. To further confirm this result, a comparison of the calculated and experimental $^{2}J_{C-H}$ heteronuclear coupling constant for C-3 and H-4 was considered. It is worth mentioning that no other significant experimental coupling constants and/or dipolar effects were observed for the tetrahydroisoquinolinic ring. A $^{2}J_{C3-H4}$ value of −5.8 Hz was obtained from a *J*-resolved HMBC[14] spectrum, which was in good accordance with the −4.3 Hz calculated value of **2b**. On the other hand, the experimental $^{2}J_{C3-H4}$ value significantly differed with respect to the calculated values for the remaining stereoisomers (−8.7 Hz for **2a**, −2.8 Hz for **2c**, and −8.9 Hz for **2d**; Figure S4 and Table S7).

Finally, the absolute configuration of **2** was analyzed by comparing the calculated and experimental circular dichroism (CD) spectra of the two possible enantiomers, 2′*S*,3*S*,4*R* and 2′*R*,3*R*,4*S*.[15,16] Starting from the previously obtained conformation of **2b**, a new optimization of the geometries was performed at the DFT level using the IEFPCM methanol model. A Boltzmann-weighted CD spectrum was calculated for 2′*S*,3*S*,4*R* and its enantiomer 2′*R*,3*R*,4*S*. As shown in Figure 5, the experimental curve closely fits with that of 2′*S*,3*S*,4*R*, thereby suggesting the absolute configuration of **2**. CD spectra were also calculated for all the other six possible stereoisomers. None of them showed significant similarity to the experimental spectrum (Figure S5). Furthermore, the hyalachelin B skeleton shows slight similarities to the known myxobacterial-derived myxochelins. These catechol-type siderophores are biosynthetically

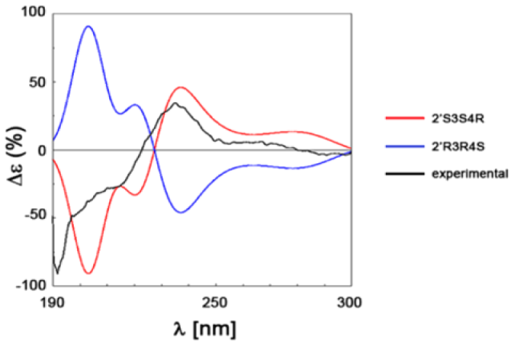

Figure 5. Comparison of experimental CD spectrum and 2′*S*,3*S*,4*R* and 2′*R*,3*R*,4*S* CD calculated spectra.

derived from L-lysine and show an *S* configuration.[17] Interestingly, our results point out an *S* configuration at C-2′, additionally supporting our analysis. The relative configurations of **1** and **3** were assumed to be identical to those of **2** because their structures and NMR data are very similar. Formally, the hyalachelins might be derived from myxochelins by the addition of phenylalanine, tyrosine, or tryptophan, respectively. How exactly this intriguing biosynthesis is achieved is currently under investigation in our laboratory.

The structural features of hyalachelins suggested that these natural products may possess iron chelating properties. Indeed, **1**−**3** showed iron chelating activity in a liquid chrome azurol S (CAS)[18] assay with EC_{50} values approximately 5-fold higher than those of myxochelin and deferoxamine (Table 2).

Table 2. Iron Chelating Activities (EC_{50}) of 1−3 and Positive Controls

siderophore	EC_{50} [μM]
1	39.4 ± 4.29
2	28.1 ± 7.32
3	30.1 ± 0.29
myxochelin B	4.6 ± 2.18
deferoxamine mesylate	6.7 ± 0.78

It has been shown that available iron in the growth medium affects the production of siderophore secondary metabolites.[19] Cultivation of strain MCy9135 in growth medium containing Fe-EDTA (20 μM) resulted in the loss of the production of **1**−**3** (Figure S2). This result demonstrates that hyalachelins are most likely biologically relevant siderophores of *H. minutum*.

Representative compound **3** was tested against *Staphylococcus aureus* and *Bacillus subtilis* on the basis of the slight structural similarities to myxochelins.[3] However, no inhibition was observed up to concentrations of 64 μg/mL. Besides, cytotoxic activity of **3** was evaluated toward HCT-116 and CHO-K1 cell lines resulting in IC_{50} values of 29.2 and 82.7 μM, respectively.

In summary, hyalachelins are a new class of catecholate siderophores that contain an unusual isoquinoline ring bearing an oxo group at C-1 and α-hydroxy acid at C-3. To our knowledge this is the first report of an 3,7,8-trihydroxy-1-oxo-1,2,3,4-tetrahydroisoquinoline-3-carboxylic acid residue present in a natural product. The relative and absolute configuration of **2** was elucidated by means of quantum mechanical calculations of NMR and CD parameters in comparison to experimental data.

The discovery of this new suite of secondary metabolites reconfirms the notion that unexplored myxobacteria are a

dx.doi.org/10.1021/ol501826a | *Org. Lett.* 2014, 16, 4130−4133

promising source of new scaffolds. It also highlights the abundant biosynthetic capabilities of these Gram-negative microorganisms.

■ ASSOCIATED CONTENT

Supporting Information

Full experimental details, purification and taxonomy of the strain, extraction and isolation of the hyalachelins, iron chelating activity test, ^{1}H and ^{13}C assignments, 1D and 2D-NMR spectra for **1**−**3**, quantum mechanical calculations of NMR parameters of **2**, and calculated CD spectra of **2a**, **2c**, and **2d**. This material is available free of charge via the Internet at http://pubs.acs.org.

■ AUTHOR INFORMATION

Corresponding Authors

*E-mail: rolf.mueller@helmholtz-hzi.de.
*E-mail: bifulco@unisa.it.

Notes

The authors declare no competing financial interest.

■ ACKNOWLEDGMENTS

We would like to acknowledge Thomas Hoffmann (HIPS) and Eva Luxemburger (HIPS) for performing the MS^n fragmentation experiment and Jennifer Herrmann (HIPS) and Viktoria Schmitt (HIPS) for bioactivity testing. S.N. is grateful to Deutscher Akademischer Austausch Dienst (DAAD) for a PhD scholarship. G.L. acknowledges fellowship support from Associazione Italiana Ricerca sul Cancro (AIRC) - Grant IG 2012 - IG_12777 - Bifulco Giuseppe. We wish to thank Prof. Dr. Qian Xiao-Ming of School of Life Science, Xiamen University for the kind gift of a soil sample. Research work in R.M.'s lab is supported by grants from the BMBF and the DFG.

■ REFERENCES

(1) Sandy, M.; Butler, A. *Chem. Rev.* **2009**, *109*, 4580−4595.
(2) Kong, X.; Hider, R. C. *Nat. Prod. Rep.* **2010**, *27*, 637−657.
(3) Kunze, B.; Bedorf, N.; Kohl, W.; Höfle, G.; Reichenbach, H. *J. Antibiot.* **1989**, *42*, 14−17.
(4) Silakowski, B.; Kunze, B.; Nordsiek, G.; Blöcker, H.; Höfle, G.; Müller, R. *Eur. J. Biochem.* **2000**, *267*, 6476−6485.
(5) Kunze, B.; Trowitzsch-Kienast, W.; Höfle, G.; Reichenbach, H. *J. Antibiot.* **1992**, *45*, 147−150.
(6) Plaza, A.; Müller, R. In *Natural Products: Discourse, Diversity, and Design*; Osbourn, A., Goss, R., Carter, G. T., Eds.; John Wiley & Sons: 2014; Chapter 6, pp 103−124.
(7) Plaza, A.; Viehrig, K.; Garcia, R.; Müller, R. *Org. Lett.* **2013**, *15*, 5882−5885.
(8) Plaza, A.; Garcia, R.; Bifulco, G.; Martinez, J. P.; Hüttel, S.; Sasse, F.; Meyerhans, A.; Stadler, M.; Müller, R. *Org. Lett.* **2012**, *14*, 2854−2857.
(9) Perez, M.; Crespo, C.; Schleissner, C.; Rodriguez, P.; Zuniga, P.; Reyes, F. *J. Nat. Prod.* **2009**, *72*, 2192−2194.
(10) Okanya, P. W.; Mohr, K. I.; Gerth, K.; Kessler, W.; Jansen, R.; Stadler, M.; Müller, R. *J. Nat. Prod.* **2014**, *77*, 1420−1429.
(11) Cimino, P.; Duca, D.; Gomez-Paloma, L.; Riccio, R.; Bifulco, G. *Magn. Reson. Chem.* **2004**, *42*, S26−S33.
(12) (a) Bifulco, G.; Dambruoso, P.; Gomez-Paloma, L.; Riccio, R. *Chem. Rev.* **2007**, *107*, 3744−3779. (b) Bagno, A.; Rastrelli, F.; Saielli, G. *Chem.—Eur. J.* **2006**, *12*, 5514−5525.
(13) Frisch, M. J.; Trucks, G. W.; Schlegel, H. B.; Scuseria, G. E.; Robb, M. A.; Cheeseman, J. R.; Scalmani, G.; Barone, V.; Mennucci, B.; Petersson, G. A.; Nakatsuji, H.; Caricato, M.; Li, X.; Hratchian, H. P.; Izmaylov, A. F.; Bloino, J.; Zheng, G.; Sonnenberg, J. L.; Hada, M.; Ehara, M.; Toyota, K.; Fukuda, R.; Hasegawa, J.; Ishida, M.; Nakajima, T.; Honda, Y.; Kitao, O.; Nakai, H.; Vreven, T.; Montgomery, J. A., Jr.; Peralta, J. E.; Ogliaro, F.; Bearpark, M.; Heyd, J. J.; Brothers, E.; Kudin, K. N.; Staroverov, V. N.; Kobayashi, R.; Normand, J.; Raghavachari, K.; Rendell, A.; Burant, J. C.; Iyengar, S. S.; Tomasi, J.; Cossi, M.; Rega, N.; Millam, N. J.; Klene, M.; Knox, J. E.; Cross, J. B.; Bakken, V.; Adamo, C.; Jaramillo, J.; Gomperts, R.; Stratmann, R. E.; Yazyev, O.; Austin, A. J.; Cammi, R.; Pomelli, C.; Ochterski, J. W.; Martin, R. L.; Morokuma, K.; Zakrzewski, V. G.; Voth, G. A.; Salvador, P.; Dannenberg, J. J.; Dapprich, S.; Daniels, A. D.; Farkas, Ö.; Foresman, J. B.; Ortiz, J. V.; Cioslowski, J.; Fox, D. J. *Gaussian 09*, revision D.01; Gaussian, Inc.: Wallingford, CT, 2009.
(14) Meissner, A.; Soerensen, O. W. *Magn. Reson. Chem.* **2001**, *39*, 49−52.
(15) Bringmann, G.; Bruhn, T.; Maksimenka, K.; Hemberger, Y. *Eur. J. Org. Chem.* **2009**, *17*, 2717−2727.
(16) Masullo, M.; Bassarello, C.; Bifulco, G.; Piacente, S. *Tetrahedron* **2010**, *66*, 139−145.
(17) Miyanaga, S.; Obata, T.; Onaka, H.; Fujita, T.; Saito, N.; Sakurai, H.; Saiki, I.; Furumai, T.; Igarashi, Y. *J. Antibiot.* **2006**, *59*, 698−703.
(18) Schwyn, B.; Neilands, J. B. *Anal. Biochem.* **1987**, *160*, 47−56.
(19) *Metal Ions in Biological Systems: Iron Transport and Storage in Microorganisms, Plants, and Animals*; Sigel, A., Sigel, H., Eds.; Dekker: New York, 1998.